

## Adiabatic compressibility of AOT [sodium bis(2-ethylhexyl)sulfosuccinate] reverse micelles: Analysis of a simple model based on micellar size and volumetric measurements

A. Amararene,<sup>1</sup> M. Gindre,<sup>1</sup> J.-Y. Le Hu  rou,<sup>1</sup> W. Urbach,<sup>2</sup> D. Valdez,<sup>1</sup> and M. Waks<sup>1</sup>

<sup>1</sup>Laboratoire d'Imagerie Param  trique, CNRS UMR 7623, 15 rue de l'  cole de M  decine, F-75006 Paris, France

<sup>2</sup>Laboratoire de Physique Statistique de l'ENS, CNRS URA 1306, 24 rue Lhomond, F-75005 Paris, France

(Received 13 April 1999)

The self-assembly of amphiphilic molecules into supramolecular aggregates involves a number of complex phenomena and forces. Recent developments of highly sensitive, densimetric and acoustic methods on small volume samples have provided novel sensitive probes to explore the physical properties of these complex fluids. We have investigated, by high precision densimetry and ultrasound velocimetry, reverse micelles of [sodium bis(2-ethylhexyl)sulfosuccinate] in oil (isooctane and decane), at increasing water concentration and at variable micellar volume fractions. The size of these spherical micelles has been determined by small angle x-ray scattering. Using these results, in the framework of the effective medium theory, we have developed a simple model of micellar compressibility, allowing the calculation of physical parameters (aggregation number, volume, and compressibility) of the surfactant monomolecular film as well as that of the micellar waters. In particular, we show that the central aqueous core designated as "free" water, located at a distance from the oil-water interacting interface, is twice as compressible as "bulk" water. One notable feature of this work is the influence of the nature of the oil on the above parameters.

PACS number(s): 62.10.+s

### I. INTRODUCTION

Water-in-oil microemulsions or reverse micelles have attracted the attention of physicists as early as 1943 [1]. Since then, many characteristics of reverse micelles have been extensively studied and documented [2,3]. Reverse micelles also display a number of versatile properties: they have been considered as effective membrane-mimetic systems [4], models of water-restrictive environment of biological relevance [5], microreactors for micellar enzymology or microchemistry [6,7], and recently a medium for membrane protein crystallization [8].

Reverse micelles can be described as water microdroplets of variable size, dispersed in nonmiscible apolar solvents and stabilized by a monolayer of surfactant. Their nonpolar tails protrude into and are solvated by the organic solvent, while their polar head groups are in direct contact with the water core that solvates them. Thus, reverse (or inverted) micelles are inside out with respect to more common micelles. The architecture of these organized molecular assemblies delineates two distinct compartments: the smallest one, on the inside, contains all the water present, while the largest one is made by the bulk organic phase. The two compartments are separated by a boundary, the monomolecular layer of surfactant, an interacting interface between oil and water. One of the most common systems used by investigators is the ternary mixture [sodium bis(2-ethylhexyl)sulfosuccinate] (AOT)–water–apolar solvent.

The size of these droplets, spherical in shape, which are thermodynamically stable structures, depends only on water concentration, defined as the water-to-surfactant molar ratio  $W_0$ . When water is added, the micelles swell, their radius increases, and the number of surfactant molecules per droplet (aggregation number) grows with the size of the droplet. As

a consequence, the water content of the system can be precisely varied and experimentally controlled. Provided  $W_0$  is held fixed, the volume fraction of the droplets can be varied without changing their shape and size. There is a wealth of information concerning reverse micelles, their structure, phase behavior [9–11], and the anomalous properties of micellar water, comprising at least two populations in rapid equilibrium: "bound" interfacial and "free," developing as hydration of the system is increased [12,13]. In contrast, information concerning adiabatic compressibility of reverse micelles in organic solvents remains scarce [14].

Recent developments in acoustic techniques (difference ultrasound velocimetry) have rendered possible high precision measurements with small solute volumes [15], in particular biopolymers [16,17] or complex fluids [18]. It is now well established that compressibility is exquisitely sensitive to solute-solvent interactions; at low solute concentration, the measured volume and compressibility properties reflect therefore the contribution of both solvent and solute intrinsic properties. A major issue in interpreting the results thus originates from the difficulty to discriminate between the intrinsic compressibility of a solute and that due to interactions occurring at the interface in contact with the solvent. An additional complexity of reverse micelles is generated by the possible interplay with different organic solvents [10]. One of the possible approaches of this interesting problem is to establish a microscopic model of the various compartments described above, which might account for experimental results.

To achieve this goal, we report here the determination of density and ultrasound velocity of AOT reverse micellar solutions, at water concentration corresponding to  $W_0$  values ranging between 0 and 30, and at variable micellar volume fraction. All experiments were carried out in isooctane and

decane for comparizon of solvent effect. The size of droplets was determined by small angle x-ray scattering (SAXS). From these results, by applying the effective medium theory, we have modeled the micellar compressibility with the help of simple geometrical considerations. By doing so, we have been able to predict the volume and compressibility of the AOT monomolecular film itself, as well as that of encased waters, in bound or sequestered states.

## II. MATERIAL AND METHODS

AOT was purchased from Sigma (SigmaUltra) 99% pure, and used after desiccation in vacuum over phosphorus pentoxide (Sicapent from Merck). Isooctane, Pro Analyti grade, was from Merck and decane >99% pure, from Sigma. Water used in this study was of MilliQ purity.

### A. Sample preparation

All the samples were prepared by weighing the solutes (surfactant and water) on a Model 1712 Sartorius balance, in precision volumetric flasks (class A  $\pm 0.04$  ml), with a precision of  $\pm 0.03$  mg. The solvents used to make up the volume at 20 °C, were either pure or organic solvents. The maximum error introduced by this procedure does not exceed the reported error limits.

### B. Volumetric measurements

The densities  $\rho(c)$  of solutions, at increasing solute concentrations  $c$ , were determined at  $25.00 \pm 0.01$  °C using the vibrating tube Anton Paar DMA 58 digital density meter. Each determination was carried out at least five times and averaged. The precision obtained is of the order of  $\pm 5 \times 10^{-3}$  kg m<sup>-3</sup>.

### C. Ultrasound velocity measurements

They were carried out on a custom-built apparatus. Ultrasound velocity is measured in two small (3 ml), identical cells enclosed in a single metal bloc thermostated at  $25 \pm 0.01$  °C. Both cells are first filled with the reference solvent, then the second cell is filled with the solution. A 10 MHz sine signal is gated by short pulses (400 ns). The issued signal drives simultaneously the emitting transducers (ceramic) of both cells and the output signals are captured by a digital scope. The apparatus is automated using a PC equipped with an IEEE interface. The final precision in ultrasound velocity determination is better than  $10^{-5}$ . Detailed characteristics of apparatus and experimental performances have been given elsewhere [18].

### D. Small angle x-ray scattering (SAXS)

Samples were filled at 22 °C in Lindeman capillaries of 1 mm diameter and sealed. The x-ray generator was a copper rotating anode machine operating at 40 kV and 25 mA. The x-ray apparent source had dimensions 0.1 mm  $\times$  0.1 mm. A vertical mirror acts as a total reflector for the  $\lambda_{K\alpha} = 1.54$  Å wavelength, eliminates shorter wavelengths of the beam and directs the x rays on the positive proportional counter. A nickel filter attenuates the  $K_{\beta}$  waves. The dimensions of the beam on the counter are 3 mm vertically and 0.3 mm hori-

zontally. The counter has a window of 3 mm height, a 50 mm useful length, and a 200  $\mu$ m spatial resolution. The distance between the sample and the counter is 802 mm [19]. The SAXS data, analyzed using the general equation for the scattered intensity derived by Guinier and Fournet [20] as described by [21], have been used to determine the water-pool radius  $R_w$ . The obtained radius and the calculated volume of the sphere include the surfactant polar head group volume of identical electronic density. The size polydispersity was estimated between 15 and 20 % according to  $W_0$  values.

## III. RESULTS AND DISCUSSION

### A. Micellar density

The density of AOT reverse micelles has been measured at the molar ratio of water-to-surfactant  $W_0 = 11$ , in two chemically distinct apolar solvents: isooctane is branched and decane is linear. Taking into account the densities ( $\rho_{oil}$ ), ( $\rho_{mic}$ ) and volume fractions ( $\phi_{oil}$ ), ( $\phi_{mic}$ ) of oil and micelles respectively, mass conservation law can be expressed as [22–24]:

$$\rho = \rho_{oil}\phi_{oil} + \rho_{mic}\phi_{mic}. \quad (1)$$

Improvements of the above expression have been obtained by including the effect of fluid viscosity and particle size. However, due to the small size of micelles studied in this work ( $< 100$  Å) and the low  $\phi$  values used in experiments, the corrective term is irrelevant [25].

$$\phi_{mic} = \frac{V_{mic}}{V}, \quad (2)$$

where  $V$  is the volume of the solution and  $V_{mic}$  the volume of micelles in the solution. The micellar concentration  $c_{mic}$  can be written as a function of mass of water and that of AOT:

$$c_{mic} = \frac{m_{AOT} + m_{H_2O}}{V}, \quad (3)$$

leading to an alternative form of Eq. (1),

$$\rho = \rho_{oil}\phi_{oil} + c_{mic}. \quad (4)$$

With the total volume fraction being

$$\phi_{mic} + \phi_{oil} = 1, \quad (5)$$

relation (1) becomes

$$\phi_{mic} = 1 - \frac{\rho - c_{mic}}{\rho_{oil}} \quad (6)$$

and

$$\rho = \rho_{oil} - \phi_{mic}(\rho_{oil} - \rho_{mic}). \quad (7)$$

If the oil density  $\rho_{oil}$  is assumed independent of the micellar volume fraction  $\phi_{mic}$ , then, using Eq. (6), one can easily calculate  $\phi_{mic}$ . We can now plot the measured density  $\rho$  of the solution, expressed in kg m<sup>-3</sup>, as a function of the micellar volume fraction  $\phi_{mic}$ . Figure 1 displays the plot at a

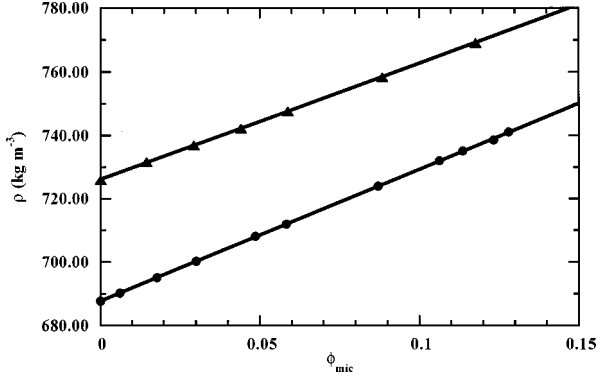


FIG. 1. Plot of the measured solution density  $\rho$ , vs the micellar volume fraction  $\phi_{\text{mic}}$ , at  $W_0 = 11$ . For  $\phi_{\text{mic}} = 0$ , the curves extrapolate to the pure solvent values. The precision of density measurements is  $10^{-5}$  and that of volume fractions is  $10^{-3}$ . In all of the figures the solvents are represented by the following symbols: (●) for isooctane and (▲) for decane.

$W_0$  value of 11: it is obvious that the increase in the solution density is linear with the increase of the micellar volume fraction. The two curves display distinctive slopes, and extrapolate at infinite dilution, close to the densities of the pure solvents. This result implies that  $\rho_{\text{mic}}$  is independent of  $\phi_{\text{mic}}$  as long as  $\phi_{\text{mic}}$  remains below 0.1 (as it is always the case throughout this work). Experimental measurements of  $\rho_{\text{mic}}$  can be carried out at various  $\phi_{\text{mic}}$  values, for example as a function of micellar size, directly related to water concentration ( $W_0$ ). From Eq. (7) one can obtain  $\rho_{\text{mic}}$  for different values of  $W_0$ . Such a plot is represented in Fig. 2; the two curves extrapolate to the values of ‘‘dry’’ AOT aggregates in each solvent for  $W_0 = 0$ . At high water concentration as  $\rho_{\text{mic}}$  decreases, the two curves have a tendency to converge.

### 1. Micellar water pool

Various experimental methods have been used to determine the variation of the micellar water pool radius  $R_w$  with the water content. Table I summarizes the results of SAXS measurements of  $R_w$  as a function  $W_0$ , which have been carried out using two different solvents. They are in good agreement with literature [7,26,27]. Note that in isooctane  $R_w$  is continuously smaller than in decane.

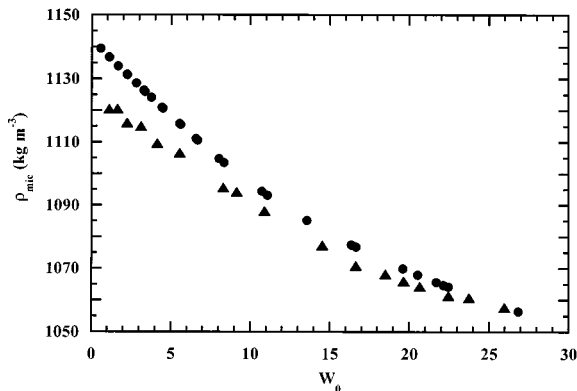


FIG. 2. Plot of the density reverse micelles  $\rho_{\text{mic}}$  vs water content  $W_0$ . The error on  $\rho_{\text{mic}}$  is estimated at  $5 \times 10^{-3}$ .

TABLE I. Aqueous core radius  $R_w$ , obtained by SAXS measurements as a function  $W_0$  in isooctane and decane. The error corresponds to  $\pm 1 \text{ \AA}$ .

$W_0$	$R_w$ ( $\text{\AA}$ )	
	Isooctane	Decane
3	8.6	8.9
5	11.7	12.3
7	14.8	15.8
9	17.9	19.2
11	21.0	22.6
15	27.2	29.5
17	30.4	32.9
19	33.5	36.4
22	38.2	41.5
25	42.8	46.7
27	45.9	50.1
30	50.6	55.2

Now, if we consider the densities and the volume fractions of water and of the surfactant AOT, one can write the mass conservation law for all micelles present,

$$\rho_{\text{mic}} = \rho_{\text{AOT}}\phi_{\text{AOT}} + \rho_{\text{H}_2\text{O}}\phi_{\text{H}_2\text{O}}, \quad (8)$$

$$\phi_{\text{AOT}} + \phi_{\text{H}_2\text{O}} = 1, \quad (9)$$

$\phi_{\text{AOT}}$  and  $\phi_{\text{H}_2\text{O}}$  being respectively the volume fractions of AOT and water within micelles. Assuming identical spherical micelles leads to

$$\phi_{\text{AOT}} = \frac{V_{\text{AOT}}}{V_{\text{mic}}} = 1 - \left( \frac{R_w}{R_w + l_c} \right)^3, \quad (10)$$

where  $l_c$  represents the average length of the surfactant tail solvated by oil taken as  $11 \text{ \AA}$ . The sum of the radius of the water pool and the length of the surfactant tail, i.e.,  $R_w + l_c$  represents a value close to the micellar hydrodynamic radius  $R_H$ , as determined in literature [28–30].

If we introduce now the concentration of AOT ( $c_{\text{AOT}}$ ) and that of water ( $c_{\text{H}_2\text{O}}$ ) in Eq. (3), one can write

$$c_{\text{mic}} = \rho_{\text{mic}}\phi_{\text{mic}} = c_{\text{AOT}} + c_{\text{H}_2\text{O}} \quad \text{with} \quad c_{\text{AOT}} = \frac{m_{\text{AOT}}}{V}. \quad (11)$$

Rearranging Eqs. (8) and (11) leads to the density of AOT monomolecular film itself,

$$\rho_{\text{AOT}} = \frac{c_{\text{AOT}}}{\phi_{\text{AOT}}\phi_{\text{mic}}}. \quad (12)$$

Note that  $\phi_{\text{AOT}}$  and  $\phi_{\text{mic}}$  can be obtained from Eqs. (10) and (6), leading to Eq. (12). We can therefore express  $\rho_{\text{AOT}}$  as a function of  $R_w$ , directly proportional to the water content  $W_0$ , as illustrated in Fig. 3. It is obvious that the density of the surfactant film decreases, down to a  $W_0$  value between 10, 12, and then reaches a different plateau value distinct for each solvent. Note that for  $W_0 = 0$ ,  $\rho_{\text{AOT}}$  is close to the value

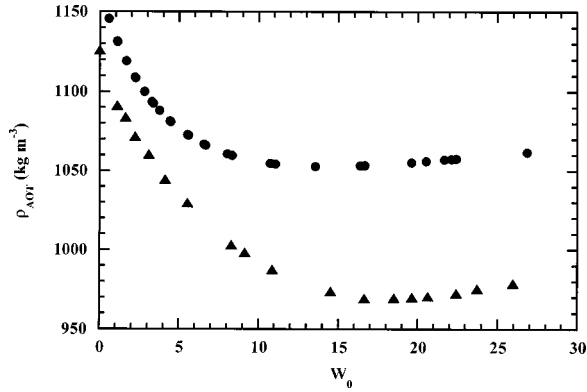


FIG. 3. Variation of the micellar AOT density  $\rho_{\text{AOT}}$  as a function of  $W_0$ . The difference between isooctane and decane levels off after  $W_0 = 12$ .

of the “dry” surfactant aggregate in each solvent [18]. Since the monolayer surfactant tails are solvated by two oils of different chemical nature, these values reflect the isooctane or decane/AOT interactions. Such effect has been related to different degrees of penetration of the surfactant chain region by the solvents, affecting the bending elasticity constant [31], possibly due to a better fit between the branched solvent chains and surfactant tails [11].

### 2. Area per surfactant polar head group

From the previous results we can deduce the variation of the surfactant polar head group area with  $W_0$ . If the volume of a spherical micelle is  $v_{\text{mic}} = \frac{4}{3}\pi R_H^3$ , and the total number of micelles in solution is  $N = V_{\text{mic}}/v_{\text{mic}}$ , the aggregation number ( $n_{\text{AOT}}$ ), i.e., the number of surfactant molecules per micelle is defined as

$$n_{\text{AOT}} = \frac{m_{\text{AOT}}}{M_{\text{AOT}}} \frac{N_{\text{av}}}{N}, \quad (13)$$

where  $M_{\text{AOT}}$  is the molecular mass of AOT (444.4 g mole<sup>-1</sup>), and  $N_{\text{av}}$  the Avogadro number. The variation of the aggregation number,  $n_{\text{AOT}}$ , as a function of  $W_0$ , is represented in Table II for isooctane and decane. The values calculated for both solvents are of the same order of magnitude, but constantly larger in decane.

The area per surfactant polar headgroup  $\sigma$  is then given by

$$\sigma(W_0) = 4\pi \frac{R_w^2}{n_{\text{AOT}}}. \quad (14)$$

The values of  $\sigma$  as a function of increasing water content  $W_0$ , are given in Table II; the agreement with values extracted from the literature is good [26,27,32].

### 3. Average volume of a water molecule

At this point, knowing the number of AOT molecules per micelle ( $n_{\text{AOT}}$ ) the number of water molecules per micelle,  $n_{\text{H}_2\text{O}}$ , will be  $W_0 n_{\text{AOT}}$ . The total volume of the water molecules in a micelle is  $v_w = \frac{4}{3}\pi R_w^3$ . One can thus estimate the average volume  $v_w$  occupied by a micellar water molecule, calculated for each value of  $W_0$ ,

TABLE II. Variation of the aggregation number  $n_{\text{AOT}}$  and of the area per surfactant polar headgroup  $\sigma$  as a function  $W_0$ .

$W_0$	$n_{\text{AOT}}$		$\sigma$ (Å <sup>2</sup> )	
	Isooctane	Decane	Isooctane	Decane
3	43	51	21	24
5	64	77	28	29
7	88	104	33	33
9	114	132	37	37
11	143	163	40	40
15	212	228	44	44
17	253	264	46	46
19	298	302	47	47
22	376	363	48	49
25	468	429	49	50
27	538	476	50	50
30	658	552	50	51

$$v_w = \frac{V_w}{n_{\text{H}_2\text{O}}} = \frac{4}{3}\pi \frac{R_w^3}{W_0 n_{\text{AOT}}}. \quad (15)$$

We have plotted in Fig. 4 the volume variation of a water molecule sequestered within an AOT reverse micelle in isooctane and decane, as a function of  $W_0$ . We observe in isooctane that the minimum molecular volume (21 Å<sup>3</sup>) is obtained for  $W_0 = 3$ , a value corresponding to the three non-freezing [13], most strongly bonded water molecules [12]. Note that according to Collins [33], those first 2, 3 water molecules hydrating the immediate surfactant sulfonate groups (SO<sup>3-</sup>), are also considered in the strongest interaction with the anion. For the highest  $W_0$  measured, it reaches in isooctane a value of about 28 Å<sup>3</sup>, close to that used by most investigators for “bulk water” (30 Å<sup>3</sup>). In decane the overall curve profile is similar to that in isooctane, although the minimum is somewhat lower and the curve does not reach the “bulk” water volume. These curves clearly indicate the influence of the solvent chemical structure, not only on micellar physical properties, but as well on the characteristics of encased water itself.

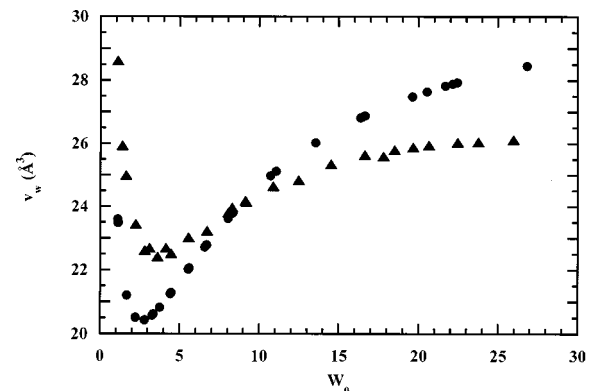


FIG. 4. Plot of the volume of a micellar water molecule as a function of  $W_0$ . Note that the minimum volume is obtained for  $W_0 = 3$ .

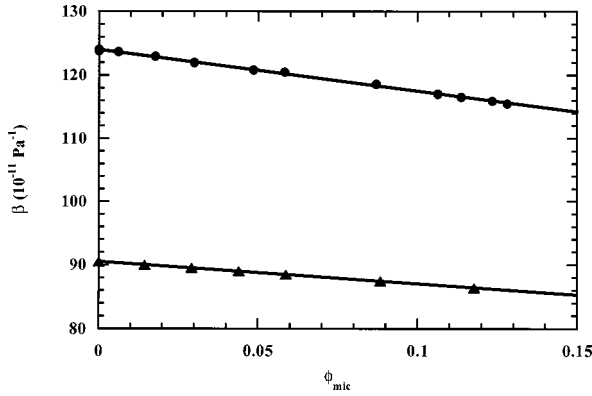


FIG. 5. Plot of solution compressibility  $\beta$  vs the micellar volume fraction  $\phi_{\text{mic}}$ , for  $W_0 = 11$ . For  $\phi_{\text{mic}} = 0$ , the curves extrapolate to compressibility of the pure solvents. The compressibility decreases linearly with  $\phi_{\text{mic}}$ . The precision of compressibility values is estimated to 1%.

### B. Micellar compressibility

Experimental determination of the density of the solution and measurements of sound velocity,  $u$ , allow the determination of adiabatic compressibility  $\beta$  of the solution using Laplace's equation,

$$\beta = \frac{1}{\rho u^2}. \quad (16)$$

In this work we make use of the effective medium theory [34], to account for the behavior of reverse micelles, since the relevant acoustic wavelength is always orders of magnitude larger than the size of micelles. We take one phase to be the continuum fluid, while the second phase consists of micellar inclusions randomly embedded in the continuous phase. Each of the constituent phases is described by parameters corresponding to the pure phase. We describe each of the constituent components, the oil phase and the inclusion phase, as a function of the relative volumes of the constituent phases, in terms of several parameters.

Thus, we can relate the solution compressibility  $\beta$  to both micellar ( $\beta_{\text{mic}}$ ) and solvent ( $\beta_{\text{oil}}$ ) compressibilities [22–24],

$$\beta = \beta_{\text{mic}}\phi_{\text{mic}} + \beta_{\text{oil}}\phi_{\text{oil}}, \quad (17)$$

with  $\phi_{\text{oil}} + \phi_{\text{mic}} = 1$ . Hence, Eq. (17) becomes

$$\beta = \beta_{\text{oil}} + \phi_{\text{mic}}(\beta_{\text{mic}} - \beta_{\text{oil}}). \quad (18)$$

In Fig. 5, we have plotted the measured solution compressibility,  $\beta$ , as a function of  $\phi_{\text{mic}}$ . At a  $W_0 = 11$ , it is obvious that the relationship is linear, the value of  $\beta$  remaining always higher in isooctane than in decane. If we assume that  $\beta_{\text{oil}}$  is independent from  $\phi_{\text{mic}}$ , we can also conclude that  $\beta_{\text{mic}}$  is independent of the micellar volume fraction,  $\phi_{\text{mic}}$ . Thus, at a given  $W_0$  (or micellar water radius,  $R_w$ ),  $\beta_{\text{mic}}$  remains constant. This result has been confirmed for different values of  $W_0$  (not shown).

From Eq. (18) one can calculate  $\beta_{\text{mic}}$  as a function of  $W_0$ . Such a plot shown in Fig. 6, displays again distinctive features for isooctane and decane. For the former, one can observe a sharp increase of the curve until  $W_0 = 10$ , which

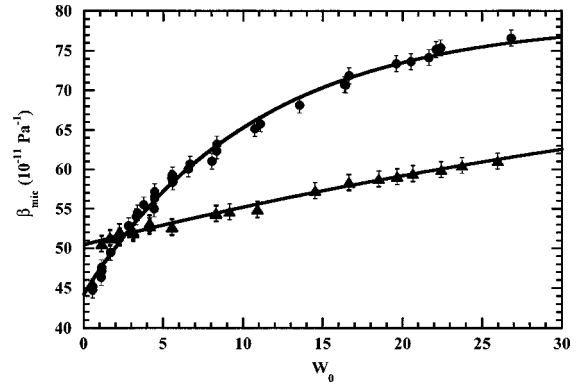


FIG. 6. Plot of micellar compressibility  $\beta_{\text{mic}}$ , as a function of  $W_0$ . The isooctane and decane curves cross around  $W_0 = 3$ . The error is  $\pm 1 \times 10^{-11} \text{ Pa}^{-1}$ .

corresponds to the upper limit of “bound” water, and then a very slow increase. For the latter solvent,  $\beta_{\text{mic}}$  displays lower values under  $W_0 = 3$ , and increases then proportionally to  $W_0$ , between 10 and 30. It is intriguing that the two curves intersect at  $W_0 = 3$ , evidencing once more the importance of the three first water molecules, very tightly bound to the surfactant polar head groups.

### C. Modeling water compressibility

The variation of  $\beta_{\text{mic}}$  as a function of  $W_0$  can be interpreted by making use of the effective medium theory, applied at the level of the micelle itself,

$$\beta_{\text{mic}} = \beta_{\text{AOT}}\phi_{\text{AOT}} + \beta_{\text{H}_2\text{O}}\phi_{\text{H}_2\text{O}}, \quad (19)$$

where  $\phi_{\text{AOT}}$  is defined by Eq. (10) and  $\beta_{\text{AOT}}$ ,  $\beta_{\text{H}_2\text{O}}$  are the respective compressibilities of AOT and micellar water.

For  $W_0 < 10$ , one can assume as a first approximation,  $\phi_{\text{AOT}} \approx 1$  and Eq. (19) shows that micellar compressibility is very close to that of the monomolecular film of AOT, so that:  $\beta_{\text{mic}} \approx \beta_{\text{AOT}}$ . We can thus plot  $\beta_{\text{mic}}$  versus the surfactant polar head group area  $\sigma$ , as given in Eq. (14). Figures 7(a) and 7(b) illustrates such a plot: there is a linear relation between compressibility and  $\sigma(W_0)$ ,

$$\beta_{\text{mic}}(\sigma) = a + b\sigma(W_0) \approx \beta_{\text{AOT}}(\sigma), \quad (20)$$

where  $a$  and  $b$  are obtained by the linear fit of  $\beta_{\text{mic}}(\sigma)$ . Figure 7 also shows that the slope  $b$  is significantly higher in isooctane than in decane, underlining once more the difference between AOT-isooctane and decane interactions.

For  $W_0 > 10$  ( $\phi_{\text{H}_2\text{O}} > 0.15$ ), it is obvious that the linear relation is no more valid for  $\beta_{\text{mic}}(\sigma)$  and the contribution of  $\beta_{\text{H}_2\text{O}}$  has to be taken into account. Eq. (19) then becomes

$$\beta_{\text{mic}}(W_0) = \beta_{\text{AOT}}(\sigma)\phi_{\text{AOT}} + \beta_{\text{H}_2\text{O}}(W_0)\phi_{\text{H}_2\text{O}}. \quad (21)$$

The above equation allows the calculation of  $\beta_{\text{H}_2\text{O}}$  as a function of the water content  $W_0$ , assuming that  $\beta_{\text{AOT}}$  varies according to Eq. (20). The results are represented in Fig. 8: for the lowest  $W_0$  studied, where water is tightly bound to the AOT sulfonate head groups, we obtain thus average values for  $\beta_{\text{H}_2\text{O}}(0) = (60 \pm 4) \times 10^{-11} \text{ Pa}^{-1}$  in isooctane and

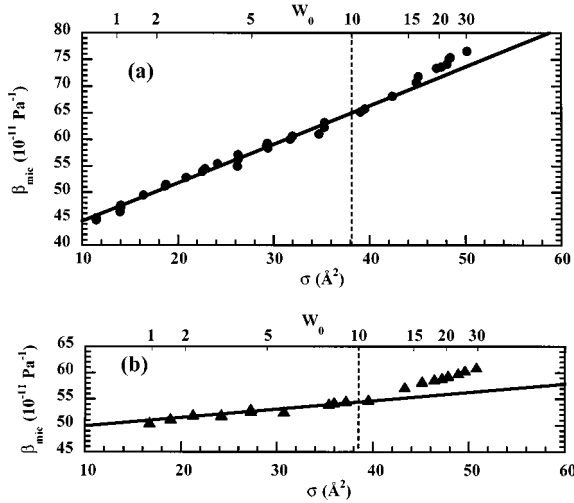


FIG. 7. Variation of micellar compressibility  $\beta_{\text{mic}}$  with the surfactant polar headgroup area  $\sigma$ . Since the relation of  $\sigma$  with  $W_0$  also depends on the nature of the solvent, (see Table I), the corresponding  $W_0$  values are indicated on the top of each curve: (a) in isooctane, (b) in decane. The relation is linear to about  $W_0 = 10$ .

$(54 \pm 4) \times 10^{-11} \text{ Pa}^{-1}$  in decane. For the highest  $W_0$  measured (in the 23, 26 range), where water is often designated as “free,” but yet remains sequestered in a restricted volume, compressibility reaches  $80 \times 10^{-11}$  and  $67 \times 10^{-11} \text{ Pa}^{-1}$  for the same solvents, respectively.

We can also model the variation of the aqueous compressibility  $\beta_{\text{H}_2\text{O}}$  as a function of  $W_0$ . Within a reverse micelle, water can be represented by a first central aqueous sphere of adiabatic compressibility  $\beta^F$ . A second external water-shell of thickness  $d$ , is in tight interaction with the surfactant anionic headgroups and is designated as “bound”; its compressibility is  $\beta^B$ . These numbers cannot be obtained experimentally, but can be extracted from our model.

By applying again the effective medium theory to the water pool of the reverse micelle, one can write

$$\beta_{\text{H}_2\text{O}}(W_0) = \beta^F \phi^F + \beta^B \phi^B, \quad (22)$$

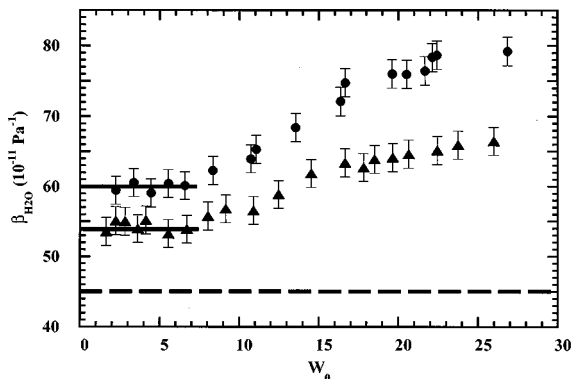


FIG. 8. Plot of the micellar water compressibility  $\beta_{\text{H}_2\text{O}}$  vs  $W_0$  in isooctane and decane. The dashed line represents the compressibility of “bulk” water. Straight lines correspond to bound water. At high  $W_0$ , water is present as a mixture of “bound” and “free” form.

Simple geometrical considerations lead to  $\phi^F = [1 - (d/R_w)]^3$  and  $\phi^B = 1 - \phi^F$ . Assuming the bound water thickness  $d = 4 \text{ \AA}$  [26], we can calculate  $\phi^F$ .

For  $W_0 < 5$  there is a general agreement [2,3] that all water present is tightly bound to the surfactant monolayer, and on the first approximation  $\phi^B \approx 1$ , consequently  $\beta^B \approx \beta_{\text{H}_2\text{O}}$ . Taking for  $\beta^B$  the values found above, i.e.,  $60 \times 10^{-11}$  and  $54 \times 10^{-11} \text{ Pa}^{-1}$  in isooctane and decane respectively, one obtains, using Eq. (22), the compressibility of the central water core at the highest water content measured ( $W_0 = 30$ ): these numbers are  $\beta^F = 85 \times 10^{-11}$  and  $67 \times 10^{-11} \text{ Pa}^{-1}$  for the two solvents. It could be intuitively expected for these values, to tend toward the compressibility of “bulk” water, but since we do not observe this behavior in Fig. 8, we can conjecture the existence of a  $\beta^F$  maximum with a subsequent decrease for much higher values of  $W_0$ , not obtained in this work due to phase instability. In any case, the above mentioned compressibilities are substantially higher than that of “bulk” water ( $45 \times 10^{-11} \text{ Pa}^{-1}$ ). In addition, at intermediate  $W_0$  values, the observed variation can be attributed to water molecules in rapid exchange between the two aqueous compartments [35]. As a matter of comparison, note that the compressibilities of pure solvents are  $121 \times 10^{-11}$  and  $90 \times 10^{-11} \text{ Pa}^{-1}$  for isooctane and decane, respectively.

#### IV. CONCLUSION

Efforts to understand the physical properties of molecular assemblies constituted of surfactant, oil, and water have led to an abundant literature. In particular the variation of the hydrodynamic radius  $R_H$  (or the radius of the water core  $R_w$ ) with the aggregation number  $n_{\text{AOT}}$ , and the surface of the polar headgroup with the molar water-to-surfactant ratio  $W_0$ , have been documented in AOT reverse micelles [2,3,36]. In the present work, we have used high precision density measurements to obtain a direct estimation of the micellar volume fraction. Using ultrasound velocity measurements, we present an approach that makes possible the interpretation of micellar adiabatic compressibility by the use of a simple model.

The first significant finding of this work is that in AOT reverse micelles, the nature of apolar solvent exerts a distinct action on the properties of the surfactant, such as aggregation number, polar headgroup area, as well as on that of the encased micellar water (volume and compressibility), be it bound or sequestered. Such effects have been related to different solvent penetration of the surfactant chain region, affecting the bending elasticity constant. Our results point also to the higher density of bound water, in agreement with observations by  $x$ -ray and neutron scattering experiments, of protein-water interface, in particular in the first hydration shell of proteins [37].

Our model has its own limitations. For example, if at a high water content, we rule out the existence of a compressibility maximum, discussed in the preceding section, this might indicate that the model is no longer valid. In addition, there are different formulations describing ultrasonic propagation in complex fluids. In this work, we have favored the simplest approach. In addition, we did not take into account the apparent polydispersity of solutions since it is at the low-

est level at  $W_0$  values, where most of our experiments have been carried out. The microemulsion clustering and the deviations of spherical shape observed by [38], occur at temperatures and  $W_0$  values higher than that reported in this work.

Another approach would consist in using hydrodynamic equation balancing momentum and continuity of the phases, with the drag of one phase with another, or multiple scattering theory [39]. An alternative treatment would be to use the variational principle [40]. Nevertheless, it has been shown that, for complex fluids with acoustic impedance of inclusions close to that of the solvent, the effective medium approach is the most convenient [39]. Indeed, the multiple scattering can be neglected for volume fractions lower than 0.15 and for particle radii lower than 8 nm at frequencies of several MHz or less.

In any case our model is operational since we have used it to extract a number of micellar parameters in good agreement with literature, and to discriminate the properties of micellar water. In summary, it has enabled us to shed light on several interesting and unsolved problems:

(i) For the lowest amounts of micellar water encapsulated ( $W_0 < 10$ ), corresponding to “bound” water, the adiabatic compressibility of the micellar solution is proportional to the AOT monolayer polar head group area, in direct contact with the above water. If these few water molecules do not contribute substantially to the overall micellar compressibility, they act as surfactant plasticizers and lubricants [41], by hydrating AOT polar head groups.

(ii) At higher water concentration ( $W_0 > 10$ ), sequestered water contributes substantially to micellar compressibility.

For upper values of  $W_0$ , our model allows one to discriminate the contribution of waters tightly interacting with the polar headgroups, from that due to “free” water, which accumulates within the center of the micelle as  $W_0$  increases. We show that the latter is about twice as compressible as “bulk” water, which is expected for water in a confined geometry [42]. Compressibility thus correlates with other physical properties of confined water, structured by anomalous hydrogen bonding and ion solvation.

(iii) The model allows one to predict the variation of the average volume of a single micellar water molecule solvating the surfactant polar head group, as a function of the water content of the system. We find the minimum molecular volume for  $W_0 \approx 3$  in both isooctane and decane, corresponding to three nonfreezing water molecules. We believe that similar events may occur in the first water solvation shell of proteins.

We expect that our results will help to elucidate new properties of these organized molecular assemblies. Such clarification should ultimately lead to a better understanding of the physical properties of biological macromolecules entrapped in the micellar aqueous core [43]. Nevertheless, further investigation will be required to fully understand the intriguing properties of this complex system.

#### ACKNOWLEDGMENTS

This research was supported by Centre National de la Recherche Scientifique (Grant No. PCV 98N21/0125). The authors are grateful to Morvan Léon for the precision of his work. They wish to thank R. Ober for his help in SAXS measurements.

- 
- [1] T. P. Hoar and J. H. Schulman, *Nature (London)* **152**, 102 (1943).
- [2] P. L. Luisi and L. J. Magid, *Crit. Rev. Biochem.* **20**, 409 (1986).
- [3] C. Oldfield, *Biotechnol. Genet. Engin. Revs.* **12**, 255 (1994).
- [4] C. Nicot, M. Vacher, M. Vincent, J. Gallay, and M. Waks, *Biochemistry* **24**, 7024 (1985).
- [5] M. Waks, *Proteins: Struct., Funct., Genet.* **1**, 4 (1986).
- [6] K. Martinek, A. V. Levashov, N. Klyachko, Y. L. Khmelnski, and I. V. Berezin, *Eur. J. Biochem.* **155**, 453 (1986).
- [7] M.-P. Pileni, *J. Phys. Chem.* **97**, 6961 (1993).
- [8] H. Wille and S. B. Prusiner, *Biophys. J.* **76**, 1048 (1999).
- [9] H.-F. Eicke, *J. Colloid Interface Sci.* **68**, 440 (1979).
- [10] B.-H. Robinson, C. Toprakcioglu, J.-C. Dore, and P. Chieux, *J. Chem. Soc., Faraday Trans. 1* **80**, 13 (1984).
- [11] P.-D. I. Fletcher, A. M. Howe, and B. H. Robinson, *J. Chem. Soc., Faraday Trans. 1* **83**, 985 (1987).
- [12] D. J. Christopher, J. Yarwood, P. S. Belton, and B. P. Hills, *J. Colloid Interface Sci.* **152**, 465 (1992).
- [13] H. Hauser, G. Haering, A. Pande, and P. L. Luisi, *J. Phys. Chem.* **93**, 7869 (1989).
- [14] L. Ye, A. Weitz, Ping Sheng, J. S. Huang, *Phys. Rev. A* **44**, 8249 (1991).
- [15] A. P. Sarvazyan, *Ultrasonics* **20**, 151 (1982).
- [16] A. P. Sarvazyan, *Annu. Rev. Biophys. Biophys. Chem.* **20**, 321 (1991).
- [17] T. V. Chalikian and K. J. Breslauer, *Proc. Natl. Acad. Sci. USA* **93**, 1012 (1996).
- [18] A. Amararene, M. Gindre, J.-Y. Le Huérou, C. Nicot, W. Urbach, and M. Waks, *J. Phys. Chem. B* **101**, 10 751 (1997).
- [19] S. Giasson, D. Espinat, T. Palermo, R. Ober, M. Pessah, and M. F. J. Morizur, *J. Colloid Interface Sci.* **153**, 355 (1992).
- [20] A. Guinier and G. Fournet, *Small Angle Scattering of X-Rays* (John Wiley and Sons, New York, 1955).
- [21] A. Merdas, M. Gindre, R. Ober, C. Nicot, W. Urbach, and M. Waks, *J. Phys. Chem.* **100**, 15 180 (1996).
- [22] A. B. Wood, *A Textbook of Sounds* (Bell and Sons, London, 1941).
- [23] R. J. Urick, *J. Appl. Phys.* **18**, 983 (1947).
- [24] A. M. Howe, A. R. Mackie, and M. M. Robins, *J. Dispersion Sci. Technol.* **7**, 231 (1986).
- [25] W. S. Ament, *J. Acoust. Soc. Am.* **25**, 638 (1985).
- [26] A. Maitra, *J. Phys. Chem.* **88**, 5122 (1984).
- [27] J. Lang, A. Jada, and A. Malliaris, *J. Phys. Chem.* **92**, 1946 (1988).
- [28] M. Zulauf and H.-F. Eicke, *J. Phys. Chem.* **83**, 480 (1979).
- [29] D. Chatenay, W. Urbach, C. Nicot, M. Vacher, and M. Waks, *J. Phys. Chem.* **91**, 2198 (1987).
- [30] S. Christ and P. Schurtenberger, *J. Phys. Chem.* **98**, 12 708 (1994).
- [31] B. P. Binks, H. Kellay, and J. Meunier, *Europhys. Lett.* **16**, 53 (1991).

- [32] H.-F. Eicke and J. Rehak, *Helv. Chim. Acta* **59**, 2883 (1976).
- [33] K. D. Collins, *Biophys. J.* **72**, 65 (1997).
- [34] P. Sheng, *Homogenization and Effective Moduli of Materials and Media*, edited by J. L. Eriksen, D. Kinderleher, R. Kohn, and J. L. Lions (Springer-Verlag, New York, 1983).
- [35] R. E. Riter, D. M. Willard, and N. E. Levinger, *J. Phys. Chem.* **102**, 2705 (1998).
- [36] H.-F. Eicke, *Top. Curr. Chem.* **87**, 85 (1980).
- [37] D. I. Svergun, S. Richard, M. H. J. Koch, Z. Sayers, S. Kuprin, and G. Zaccai, *Proc. Natl. Acad. Sci. USA* **95**, 2267 (1998).
- [38] G. J. M. Koper, W. F. C. Sager, J. Smeets, and D. Bedeaux, *J. Phys. Chem.* **99**, 13 291 (1995).
- [39] A. H. Haracker and J. A. G. Temple, *J. Phys. D* **21**, 1576 (1988).
- [40] R. L. Weaver, *Wave Motion* **7**, 105 (1985).
- [41] L. D. Barron, L. Hecht, and G. Wilson, *Biochemistry* **36**, 13 144 (1997).
- [42] A. P. Minton, *Biophys. J.* **68**, 1311 (1995).
- [43] A. Amararene, M. Gindre, J.-Y. Le Huérou, C. Nicot, M. Waks, and W. Urbach, *Biophys. J.* **76**, A104 (1999).